ISSN 2229-5518

Performance Study of Photovoltaic DC Water Pumping System with Maximum Power Point Tracking

F. M. Bendary, Ebtisam. M. saied, Wael A. Mohamed, Z. E. Afifi

Abstract—DC photovoltaic pumping system is presented in this paper. Solar DC pump needs less solar panels to run than the AC pump. The system is divided into three parts; photovoltaic (PV) array, boost converter and permanent magnet (PM) dc motor-pump set. Solar cells have nonlinear I-V characteristics, efficiency of PV module is low and output power depends on solar isolation Level and ambient temperature. A great loss of power is due to mismatch of source and load. So to extract the maximum power delivered to the load from PV array, MPPT is implemented in the boost converter circuit. Each part of the system is modelled. The system is simulated using Matlab/Simulink .The proposed system is studied with and without maximum power point tracking conditions. The results show a very good performance and efficiency of the overall system when using MPPT compared with direct coupling. The system is studied under various climatic conditions.

Index Terms— Photovoltaic array, Boost converter, DC motor- pump, Maximum power point tracking (MPPT) of PV system.

1 Introduction

Water pumping is one of the most important applications of photovoltaic (PV) standalone systems particularly in rural areas [1]. The most important problems in solar technology are low conversion efficiency (10% to 16% efficiency for commercially available amorphous silicon solar cells) and the presence of highly non-linear I-V characteristics which depend on temperature and insolation level. When a dc motor is directly connected to a photovoltaic array, the operating point of the PV is very far from its maximum power point (MPP)[2,3].Further, due to mismatch between the operating point and maximum power point (MPP) of the solar cells, the power available from the PV array is not fully extracted. In order to extract the maximum power, the PV array must be capable of tracking the maximum power point that varies with irradiance and temperature. This method is commonly named as a maximum power point tracking (MPPT) technique. The main function of MPPT technique is to achieve maximum power from a PV system [4]. There is a large number of algorithms that are able to track MPP of a PV module have been proposed to solve the problem of efficiency. The most common methods are the perturb and observe (P&O) and the incremental conductance (InCond). The first method is popular due to its hardware simplicity [5]. The second InCond method has a great accuracy with good flexibility to rapidly varying climatic conditions. But both methods have drawbacks and need enhancements to be more accurate [6]. Nowadays, intelligent systems are progressively used such as neural network and fuzzy logic MPPT techniques [7]. Artificial Neural Network (ANN), Fuzzy Logic Controller (FLC) and adaptive MPPT controllers-based neuro-fuzzy inference system (ANFIS) based techniques are implemented [8]. The purpose of this paper is to study and compare advantages, shortcomings and execution efficiency for the overall system of water pumping with and without MPPT under varaiant climatic conditions. Matlab/Simulink is used in this paper to implement the modeling and simulations tasks, and to compare execution efficiency and accuracy for the overall system and every stage in it. In this paper, PV array is modelled with its parameters extracted based on data-sheet and the boost converter is controlled using ANFIS algorithm for maximum power point tracking. Boost converter is designed to work in CCM.

This paper is organized as follows. Section 1 is the introduction which includes the main motivationthe purpose of this paper. Section 2 views and illustrates the propsed system configuration and its parts individually. Sections 3 simulates, analyzes and compares the performance and efficiency of the photovoltaic water pumping system with and without MPPT. The summary and conclusion are given in Section 6.

2 System Description

The proposed system is divided into four major parts (a) The Solar PVarray system (b) Power electronics DC-DC boost converter (c) MPPT technique (d) PM dc motor pump set. The schematic diagram of the complete system is shown in Fig.1.

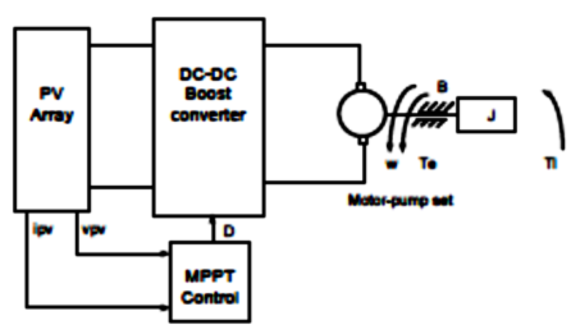

Fig. 1. System configuration schematic diagram.

ISSN 2229-5518

2.1 Photovoltaic Array Modeling

The voltage-current characteristic equation of a solar cell is given in (1).

$$I = I_{ph} - I_s \exp((V + IR_s)/(KT_c A)) - (V + IR_s)/R_{sh} \tag{1}$$

Where I_{ph} is a light-generated current or photocurrent, I_s is the cell saturation of dark current, q= (1.6*10^{-19}C) is an electron charge, k= (1.38*10^{-23} J/k) is a Boltzmann's constant, Tc is the cell's working temperature, A is an ideality factor, R_{sh} is a shunt resistance, and R_s is a series resistance. The electrical circuit representing a solar cell is shown in Fig.2. The parameters of SOLKAR 36W module, choosen for simulation, are tabulated in Table.1. Using series parallel combinations as follows (Ns= 5 & Np=6) from the module to generate power higher than 1kW at (Tac=25ºC and R= 1kW/m²)

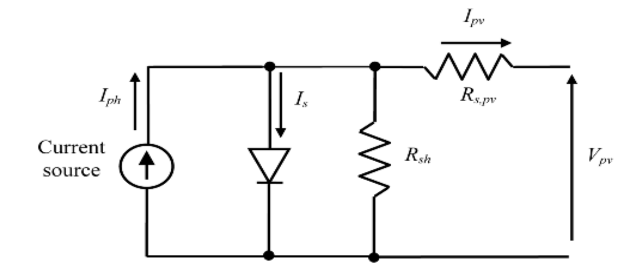

Fig. 2. Equivalent circuit of photovoltaic cell.

TABLE 1
PARAMETERS OF SOLKAR 36W MODULE

Description	Parameter
Maximum Power	P_{Max}= 40.9081 W
Voltage at Maximum Power	V_{MPP}= 17.16 V
Current at Maximum Power	I_{mp}=2.3839 A
Short Circuit Current	I_{SC}= 2.55 A
Open Circuit Voltage	V_{OC}=21.24 V
Short Circuit Current Temperature Coefficient	0.0017 A/ºC
Open Circuit Voltage Temperature Coefficient	-73e-3 V/ºC
N_S	36
N_P	1
A	1.6

2.2 Boost Converter Design

The maximum power point tracking is basically a load matching problem. In order to change the input resistance of the panel to match the load resistance, a DC-DC converter is required (by varying its duty cycle). The boost converter is capable of producing a dc output voltage (Vo) greater in magnitude than the dc input voltage (Vs). The circuit topology for a boost converter is as shown in Fig.3. The conversion ratio is given in (2).

$$V_o/V_{pv} = I_{pv}/I_o = 1/(1-d) \tag{2}$$

Where I_{pv} is the input current of the converter, duty cycle d = Ton /T and T=Ton+Toff , with its range $(0 \le d \le 1)$.

The designed boost converter parameters are as follows (L=5mH, Ci=100µF, Co=100µF and Fs=10 kHz)

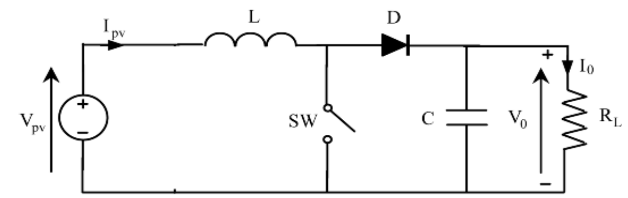

Fig. 3. Boost Converter.

2.3 DC Water Pump Modeling

DC pump motor is modeled. SIMULINK is chosen for this purpose because it offers a tool called "SimPowerSystems" which facilitates modeling of DC motors with its DC machine tool box. PM dc motor can be described in (3),(4),(5) and (6). Also centrifugal pump is described in (7).

$$V_a = i_a R_a + L_a (di_a)/dt + E_b \tag{3}$$

$$E_b = K_b w_m \tag{4}$$

$$T_e = J (dw_m)/dt + Bw_m + T_1 \tag{5}$$

$$T_e = K_e i_a \tag{6}$$

$$T_1 = K_p w_m^2 \tag{7}$$

Where:

V_a armature voltage
i_a armature current
R_a armature resistance
L_a armature inductance
E_b motor back-emf
K_b back-emf constant(V.sec/rad)
w_m motor speed(rad/s)
T_e electromagnetic torque(N.m)
J moment of inertia(Kg/m²)
B viscous friction coefficient (N.m.sec/rad)
T_1 load torque(N.m)
K_e torque constant(N.m/A)
K_p the pump constant (N.m. (sec/rad)²)

Parameters of motor-pump set used in the study are tabulated in Table 2.

TABLE 3
PARAMETERS OF MOTOR PUMP

Armature resistance(R_a)	1.254 Ω
Armature inductance(L_a)	3.49 mH
Back-emf constant (K_b = K_e)	0.333 V.sec/rad
Viscous friction coefficient(B)	0.0008 N.m.sec/rad
Moment of inertia(J)	0.004 Kg/ m²
Armature voltage(V_a)	135 V
Pump constant(K_p)	1.9 10-5 N.m. (sec/rad) ²

3 Performance Study of PM DC Motor Pump

To model a permanent magnet DC motor, the SIMULINK model applies a constant field, as shown in Fig. 4. Since the water pump is a centrifugal type, the load torque is a function of the motor speed. The voltage source applies a 0-200V ramp at the rate of 1V per second.

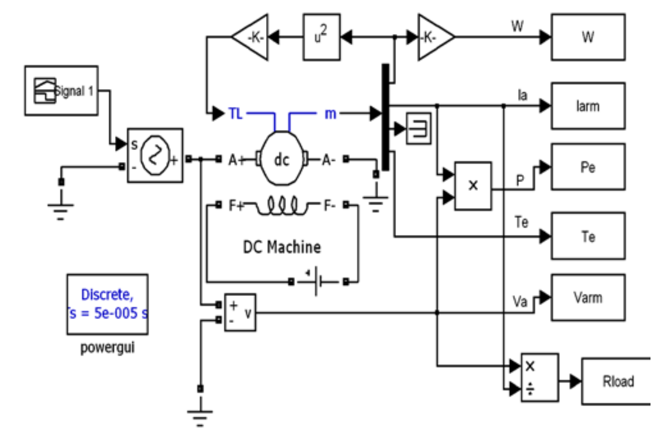

Fig. 4. SIMULINK model of permanent magnet DC pump motor.

3.1 Direct Coupling between PV Array and Motor-Pump

At direct coupling, the system operates at the intersection point between the I-V curves of the PV array and the load-line as seen in Fig.5 and Fig.6. It is obvious from the curves that the system operates far from maximum power points which led to lower energy utilization and efficiency.These operating points obtained from curves are called the expected points and tabulated in Table 4. The results under actual direct coupling match approximately the expected values from I-V curves under various climatic conditions. These actual values are tabulated in tha same table in order to compare the actual values with the expected ones as a comparative study for realizing the model and showing how it runs accurately.

TABLE 4

Comparison between The Actual and Expected operating points at direct coupling

	Tac	R	V_{Array}(V)	P_{Array}(W)	$V_{Armature}$(V)	$I_{Armature}$(A)	Motor Speed(rpm)	Torque (N.m)
Expected	25	0.4	89.83	396.1	89.83	4.41	2439	1.455
Actual			89.8	396.2	89.8	4.45	2438	1.46
Expected	25	0.6	96.36	480.5	96.36	4.987	2607	1.646
Actual			96.33	480.8	96.33	4.989	2606	1.649
Expected	25	0.8	100.1	534.1	100.1	5.332	2703	1.76
Actual			100.1	534.2	100.1	5.334	2703	1.765
Expected	25	1	102.6	571.9	102.6	5.568	2767	1.838
Actual			102.6	571.6	102.6	5.566	2767	1.837
Expected	50	1	93.22	438.6	93.22	4.706	2527	1.553
Actual			93.19	438.4	93.19	4.706	2527	1.554
Expected	75	1	83.71	326.3	83.71	3.897	2281	1.286
Actual			83.76	326.3	83.76	3.896	2281	1.286

Under fixed radiation, the following parameters, PV array output power and voltage, armature current ,motor speed and the electro-magnetic torque, are simulated and seen in the Figs. 7,8,9,10,11. The same simulations repeated under constant temperature in Figs.12,13,14,15 and 16 respectively.

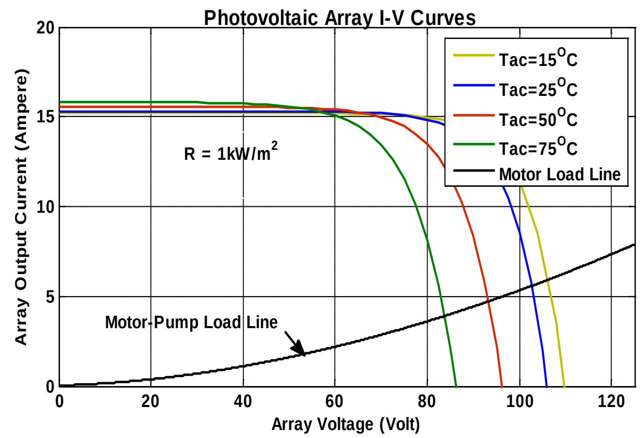

Fig. 5. Array I-V curves with constant radiation and varying temperature.

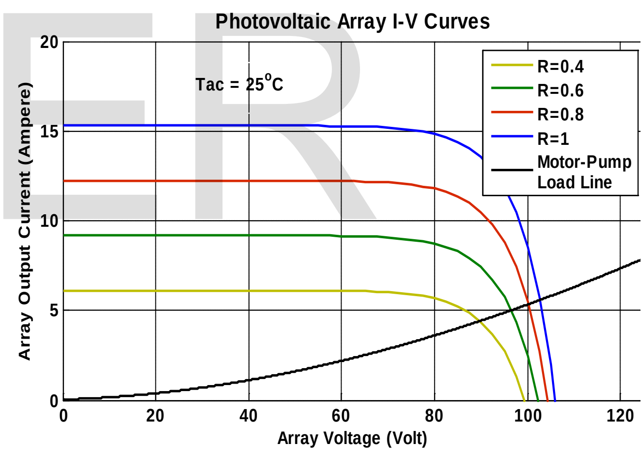

Fig. 6. Array I-V curves with constant temperature and varying radiation.

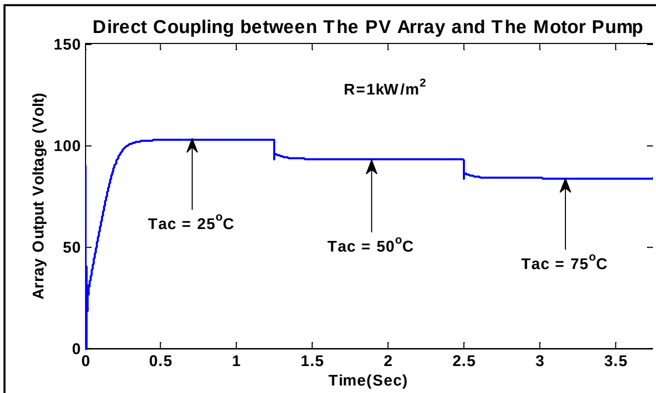

Fig. 7. Array output voltage (armature voltage).

ISSN 2229-5518

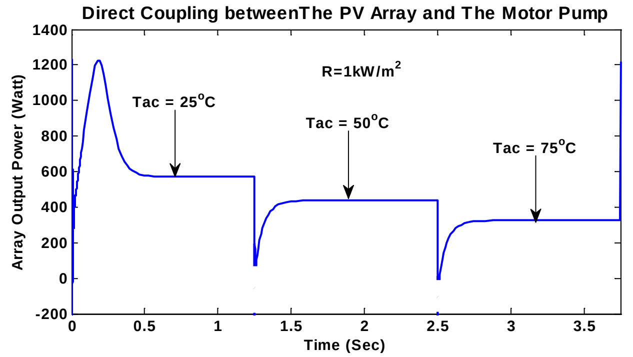

Fig. 8. Array power.

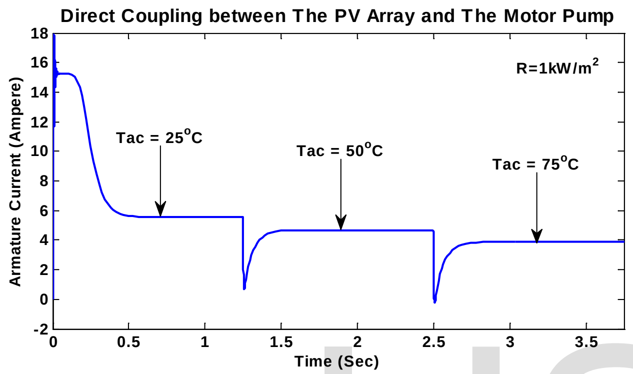

Fig. 9. Armature current.

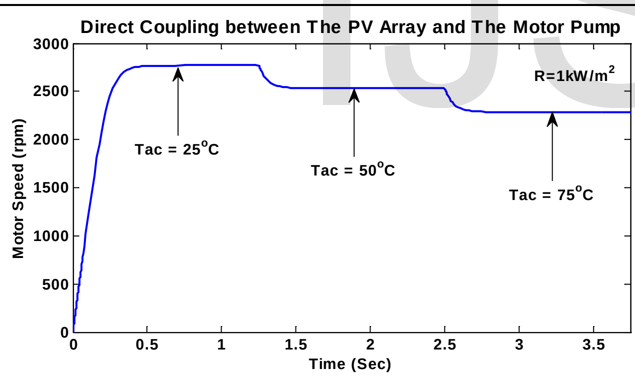

Fig. 10. Motor speed.

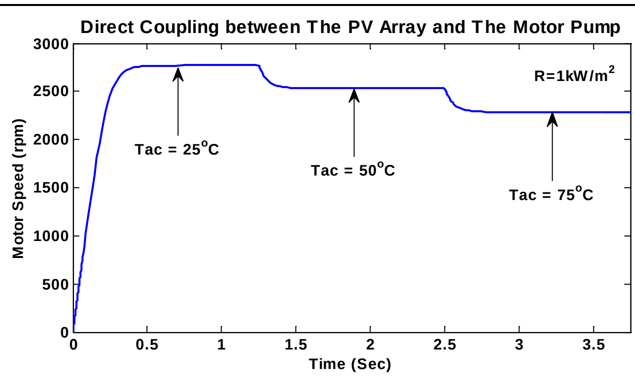

Fig. 11. Electromagnetic Torque.

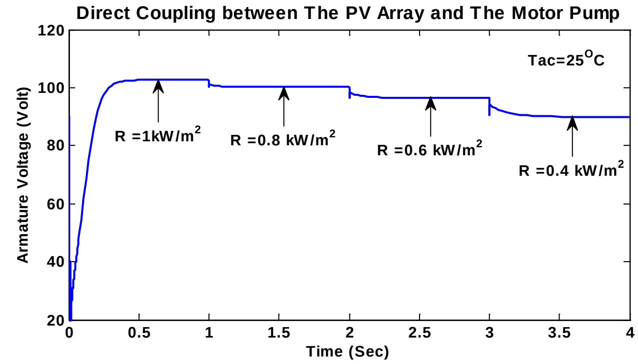

Fig. 12. Armature voltage (Array voltage).

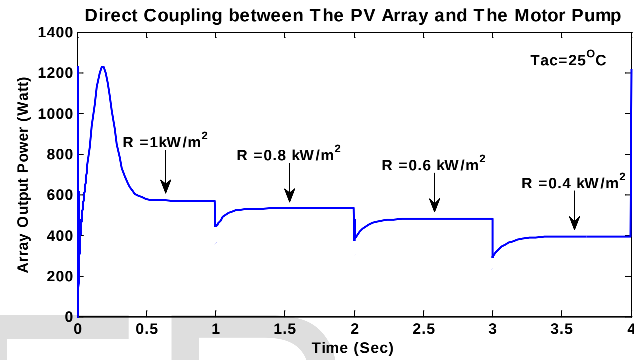

Fig. 13. Array power.

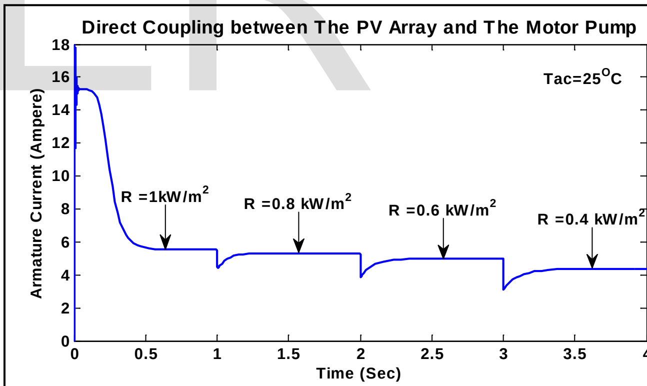

Fig. 14. Armature current.

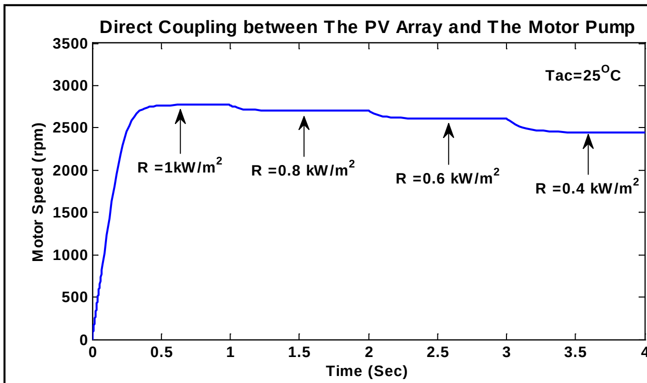

Fig. 15. Motor speed.

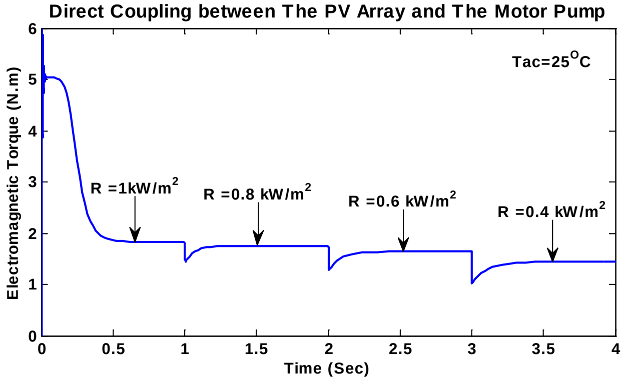

Fig. 16. Electromagnetic torque.

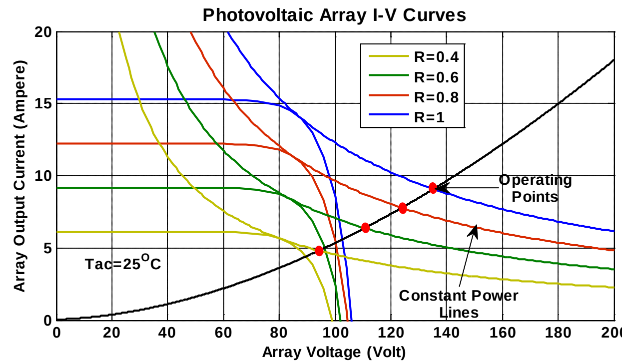

Fig. 18. Array I-V curves with constant power lines at Tac=25°C

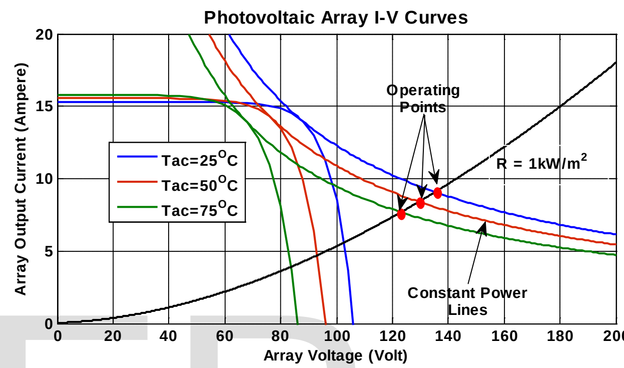

Fig. 19. Array I-V curves with constant power lines at R=1kW/m²

The efficiency of the motor pump, under direct coupling (i.e without MPPT), is calculated in Table 5. The Table shows that the efficiency is very poor without using MPPT.

TABLE 5

THE EFFICIENCY OF THE MOTOR PUMP WITHOUT MPPT.

R (kW/m²)	0.4	0.6	0.8	1	1	1
Tac (°C)	25	25	25	25	50	75
Ppv(max) (Watt)	453.48	705	964.57	1228.99	1088.33	945.42
Pm (Watt)	372.75	450.01	499.6	532.23	411.23	307.18
η(System) = Pm / Ppv	82.2%	63.8%	51.8%	43.3%	37.8%	32.5%

3.2 MPPT Coupling between PV Array and Motor-Pump

The presence of MPPT converter is needed essentially for load matching between the load and the PV array. So the power converter is always used for load matching case in MPPT techniques. The proposed model using MPPT is shown in Fig.17. The used MPPT is ANFIS algorithm used to generate reference V_{MPP} and from which the duty cycle is obtained.

In order to locate the appropriate operating points, they are the intersection points between the motor pump load line and the constant maximum power line as seen in Figs.18 and 19. Ideally the power line should be the maximum power point of the array under the same condition according to (8);

$$P_i = P_o = V_{MPP}\, I_{MPP} = V_{boost}\, I_{boost} \qquad (8)$$

Similarly comparative study between expected values from intersections and actual values of the operating points are tabulated in Table 6. Under fixed radiation, the following parameters, PV array output power and voltage, armature voltage, power and current, motor speed and the electro-magnetic torque, are simulated and seen in the Figs. 20,21,22,23,24,25 and 26 respectively. The same simulations repeated under constant temperature in Figs.26, 27, 28, 29,30,31,32 and 33 respectively. The efficiency of the motor pump, under MPPT coupling, is calculated in Table 7. The Table shows that the efficiency of the overall system is much higher with using MPPT.

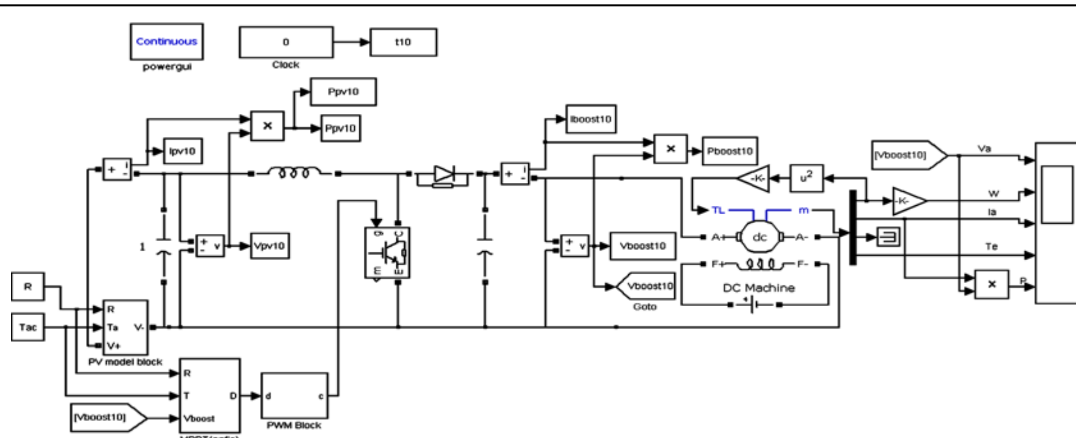

Fig. 17. The SIMULINK model at MPPT coupling between the PV array and the motor pump.

TABLE 6
COMPARISON BETWEEN THE ACTUAL AND EXPECTED OPERATING POINTS AT MPPT COUPLING

	Tac	R	$V_{PV(max)}$ (V)	$P_{PV(max)}$ (W)	$V_{(boost)}$ Armature (V)	$D_{optimum}$	$I_{Armature}$ (A)	Motor Speed(rpm)	Torque (N.m)
Expected	25	0.4	80	453.4797	94.35	0.1521	4.806	2556	1.586
Actual			**79.68**	**453.3**	**94**	**0.151**	**4.81**	**2555**	**1.59**
Expected	25	0.6	82.5	704.9958	110.7	0.2574	6.365	2972	2.1
Actual			**82.43**	**705**	**110.5**	**0.2554**	**6.37**	**2972**	**2.19**
Expected	25	0.8	85	964.569	124.04	0.3147	7.777	3307	2.566
Actual			**85.05**	**964.6**	**124**	**0.314**	**7.778**	**3306**	**2.568**
Expected	25	1	87.5	1228.993	135.4	0.3538	9.074	3589	2.995
Actual			**87.42**	**1229**	**135.3**	**0.353**	**9.077**	**3588**	**2.997**
Expected	50	1	77.5	1088.325	129.6	0.402	8.401	3445	2.772
Actual			**77.33**	**1088**	**129**	**0.401**	**8.405**	**3444**	**2.777**
Expected	75	1	67.5	945.4233	123.1	0.4517	7.673	3284	2.532
Actual			**67.48**	**945.4**	**123.0**	**0.45**	**7.677**	**3283**	**2.537**

TABLE 7
THE EFFICIENCY OF THE MOTOR PUMP WITH MPPT.

R (kW/m²)	**0.4**	**0.6**	**0.8**	**1**	**1**	**1**
Tac (°C)	**25**	**25**	**25**	**25**	**50**	**75**
Ppv (Watt)	*453.3*	*705*	*964.6*	*1229*	*1088*	*945.4*
Pboost (Watt)	*452.14*	*703.9*	*964.5*	*1228.12*	*1084.25*	*944.3*
Pm (Watt)	*425.4*	*681.6*	*889*	*1126.1*	*1001.5*	*872.2*
η(Boost) = Pboost/Ppv	*99.74%*	*99.84%*	*99.99%*	*99.93%*	*99.66%*	*99.88%*
η(Pump) = Pm/Pboost	*94.09%*	*96.83%*	*92.17%*	*91.69%*	*92.37%*	*92.36%*
η(System) = Pm / Ppv	*93.85%*	*96.68%*	*92.16%*	*91.63%*	*92.05%*	*92.26%*

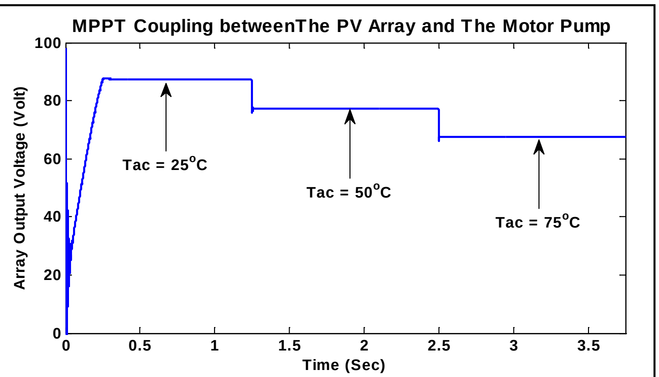

Fig. 20. Array voltage.

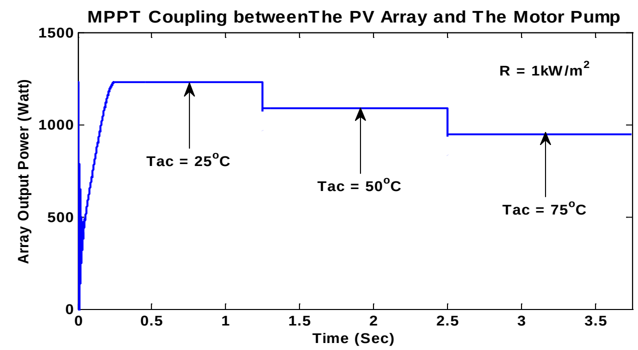

Fig. 21. Array power.

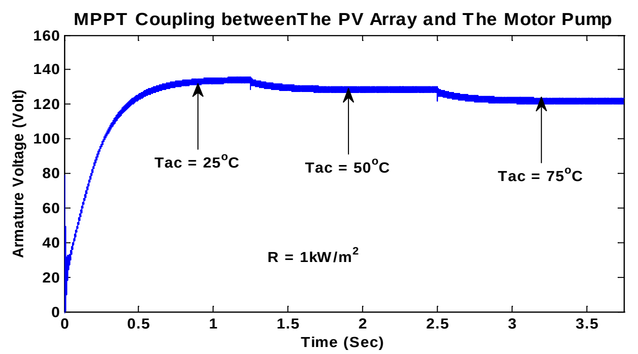

Fig. 22. Armature voltage (Boost output voltage).

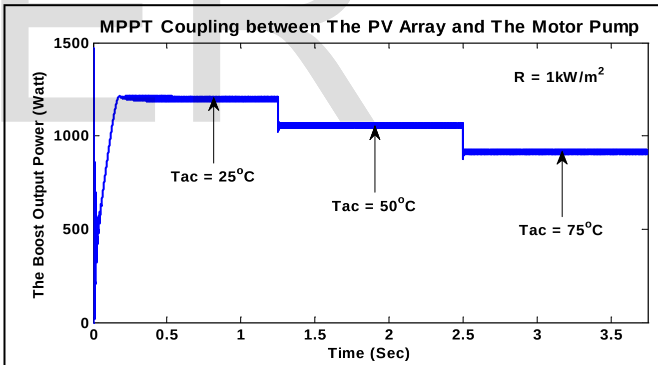

Fig. 23. Boost power.

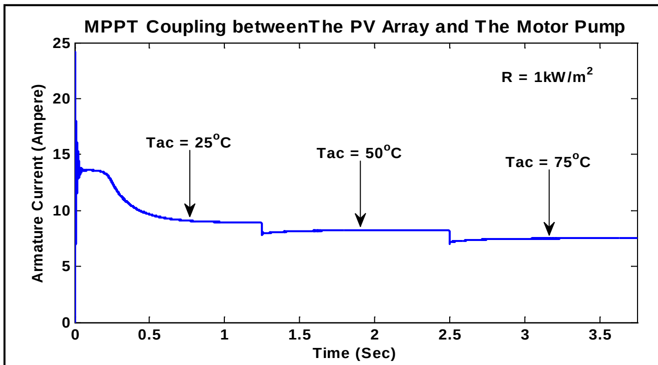

Fig. 24. Armature current.

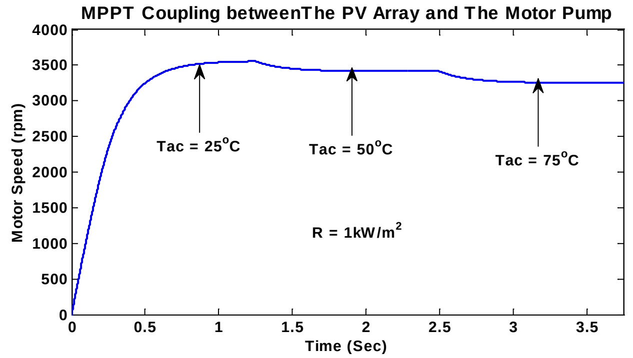

Fig. 25. Motor speed.

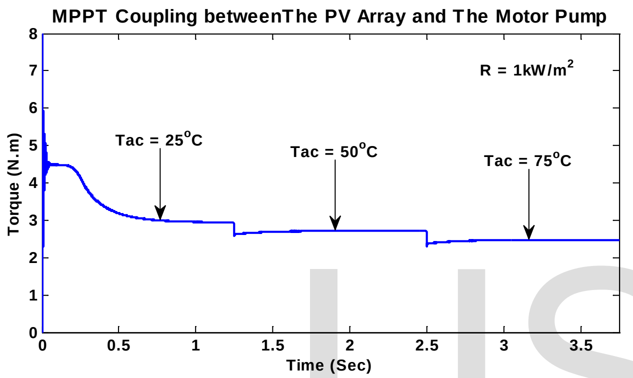

Fig. 26. Electromagnetic torque.

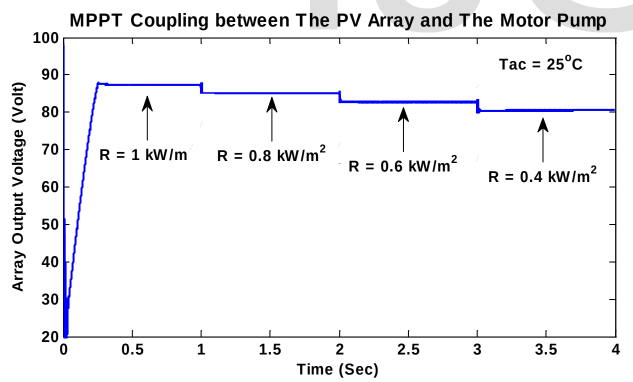

Fig. 27. Array voltage.

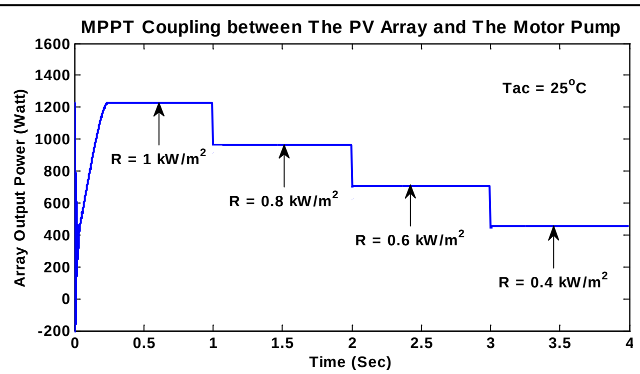

Fig. 28. Array power.

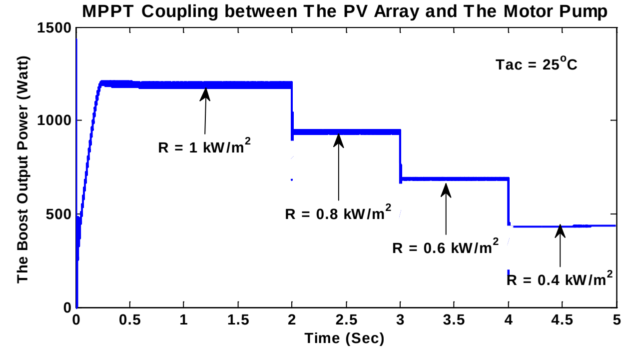

Fig. 29. Boost output power.

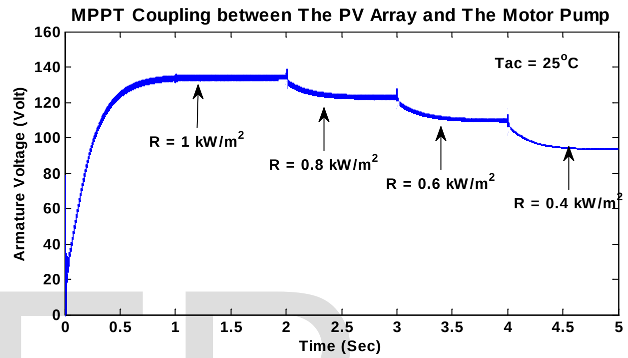

Fig. 30. Boost output voltage (Armature Voltage)

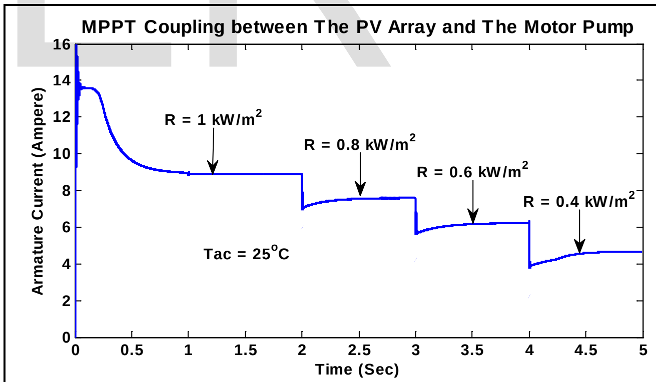

Fig. 31. Armature current

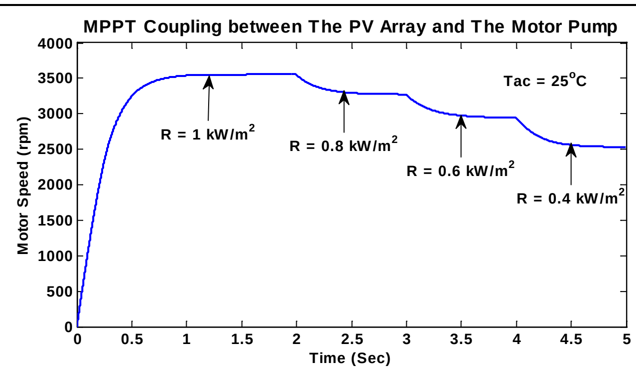

Fig. 32. Motor speed.

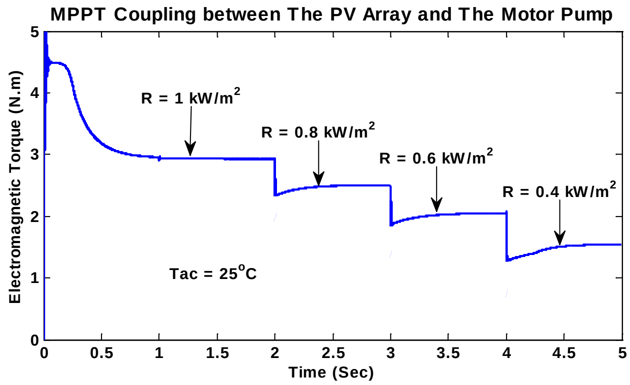

Fig. 33. Electromagnetic torque.

4 Conclusion

In this thesis, an accurate model for photovoltaic water pumping system is proposed; consisting of PV array, boost converter and PM dc motor-pump set. The system is studied under direct coupling and MPPT conditions. The system performance with different atmospheric conditions of temperature and radiation is analyzed. The Overall system efficiency under direct coupling is very low compared with that using MPPT. MPPT technique used in this thesis was ANFIS which proves how it controls the duty cycle effectively. Simulation results show a very good performance, and match approximately system solution obtained using expected points under different atmospheric conditions.

References

[1] M. A. Elgendy, B. Zahawi, and D. J. Atkinson, “Comparison of directly connected and constant voltage controlled photovoltaic pumping systems,” IEEE Trans. Sustain. Energy, vol. 1, no. 3, pp. 184–192, Oct. 2010.

[2] J. Gonzalez-Llorente, E. I. Ortiz-Rivera, A. Salazar-Llinas and E. Jimenez-Brea, “Analyzing the optimal matching of DC motors to photovoltaic modules via DC-DC converters,” Applied Power Electronics Conference and Exposition(APEC), Twenty-Fifth Annual IEEE, Palm Springs, CA, pp. 1062 – 1068, 18 march 2010.

[3] M. A. Elgendy, B. Zahawi, D. J. Atkinson and D. Giaouris “Dynamic behaviour of DC motor-based photovoltaic pumping systems under searching MPPT algorithms,” POWERENG 2009, Lisbon, Portugal, March 18 -20 ,2009, pp 413-418 .

[4] M. A. S. Masoum, H. Dehbonei and E. F. Fuchs, "Theoretical and Experimental Analyses of Photovoltaic Systems with Voltage and Current Based Maximum Power Point Tracking," IEEE Trans. OnEnergy Conversion., vol. 17, no. 4, pp. 514-522, Dec. 2002.

[5] B. Simpson, et al, “Title of paper goes here if known,” unpublished. N. Femia, G. Petrone, G. Spagnuolo, andM. Vitelli, “Optimization of perturb and observe maximum power point tracking method,” IEEE Trans. Power Electron., vol. 20, no. 4, pp. 963–973, Jul. 2005.

[6] Z. Yan, L. Fei, Y. Jinjun, and D. Shanxu, “Study on realizing MPPT by improved incremental conductance method with variable step-size,” in Proc. IEEE 3th Ind. Electron. Appl. Conf., 2008, pp. 547–550.

[7] Y. C. Kuo, T. J. Liang and J. F. Cben, "Novel Maximum Power Point Tracking Controller for Photovoltaic Energy Conversion System,"IEEE Transactions on Industrial Electronics, vol. 48, no. 3, pp. 594-601, Jun.2001.

[8] C. A. Otieno, G. N. Nyakoe, and C. W. Wekesa, “A neural fuzzy based maximum power point tracker for a photovoltaic system,” in Proc. IEEE Conf. (AFRICON’09), Nairobi, Kenya, Sep. 23–25, 2009, pp. 1–6.